Journal of Building Engineering 48 (2022) 103904

Contents lists available at ScienceDirect

Journal of Building Engineering

journal homepage: www.elsevier.com/locate/jobe

Improved strength development and frost resistance of Portland cement ground-granulated blast furnace slag binary binder cured at 0 °C with the addition of calcium silicate hydrate seeds

Ahmad Alzaza, Katja Ohenoja, Mirja Illikainen *

Fibre and Particle Engineering Research Unit, Faculty of Technology, University of Oulu, P.O. Box 4300, 90014, Oulu, Finland

ARTICLE INFO

Keywords:
Pozzolanic reaction
Low curing temperature
Nucleation
Selective dissolution
Calcium silicate hydrate seeds

ABSTRACT

Low ambient temperatures drastically decelerate the strength development of cementitious materials, which shortens the construction season in cold regions. The use of ground-granulated blast furnace slag (GGBFS) in concreting works is usually avoided in winter because of its slower hydration rate relative to Portland cement (PC). In this study, the impacts of calcium silicate hydrate (C-S-H) seeds on the strength development and reaction rate of PC/GGBFS binders cured at 0 °C were investigated. The results showed that the addition of C-S-H seeds can efficiently compensate for the strength loss caused by replacing PC with GGBFS, and this effect is more obvious at a lower GGBFS content (30%) than at a high content (50%). Better frost resistance was gained in the seeded binder containing 30% GGBFS than in the pure PC binder. The enhanced compressive strength and frost resistance in the seeded binary binder were attributed to the accelerated PC reaction rate, enhanced pozzolanic reaction rate and degree of GGBFS, and increased amount of pore-filling hydration products due to the nucleation effect of the C-S-H seeds.

1. Introduction

Cold weather is among the main challenges facing the construction industry in cold regions. Low ambient temperatures retard the early reaction process and strength gain of cementitious materials, thereby increasing the need for heating systems, delaying framework removal, and extending construction schedules. The American Concrete Institute (ACI) defines weather as "cold weather" when the air temperature is below 4 °C for more than three consecutive days and is not higher than 10 °C for 12 h [1]. These weather conditions last for at least six months in cold regions, drastically shortening the construction and infrastructure renovation season. This slows down infrastructure and urban development in cold areas considerably.

The curing temperature is a critical factor in the hydration process of Portland cement (PC) and supplementary cementitious materials (SCMs) [2,3]. As the curing temperature rises, the hydration of PC and SCMs proceed at a faster rate and vice versa. The curing temperature especially affects early-age strength development. Nmai [4] and Soutsos et al. [5] showed that despite the negligible impacts of low curing temperatures (0–10 °C) on the late (>28 d) compressive strength of PC-based binder, they significantly slowed down the early strength development rate and prolonged setting time. However, when winter construction works are unavoidable, rapid setting and hardening of PC are usually used to boost early strength development and accelerate the construction schedule. Unfortunately, these special PC types are known for their high prices, embodied energy, and carbon dioxide (CO_2) emissions

* Corresponding author.
E-mail address: Mirja.Illikainen@oulu.fi (M. Illikainen).

https://doi.org/10.1016/j.jobe.2021.103904
Received 10 October 2021; Received in revised form 29 November 2021; Accepted 15 December 2021
Available online 18 December 2021

[6,7]. These conflict with the economic interests of the construction industry in cold regions, resulting in a reluctance of contractors to undertake winter construction works.

The environmental impact and cost of concrete production can be considerably reduced by decreasing the PC content in concrete by increasing the fraction of environmentally friendly SCMs [8,9]. The PC/SCMs blends offer several benefits, such as better durability properties (e.g., frost resistance, carbonation, and acid/sulphate attacks) and higher late compressive strength in comparison with PC-based binders [9–14]. However, their low early reaction rate delays early strength gain, which conflicts with winter concreting requirements. Soutsos et al. [5] showed that the reaction of ground-granulated blast furnace slag (GGBFS) is more sensitive to the curing temperature than PC and the deceleration effects of low temperature are severer on the reaction rate between GGBFS and calcium hydroxide liberated from the hydration of PC fraction (i.e., slower pozzolanic reaction rate). They reported a 64% reduction in the compressive strength of the 3 d-old mortar prepared with 50% PC and 50% GGBFS (wt.% of binder) when the curing temperature dropped from 20 °C to 10 °C, while only a 19% reduction was calculated in the 100% PC-based mortar. Therefore, the wide-scale use of SCMs in cold weather conditions has been restricted.

Recently, several studies have aimed to enhance the reactivity of PC/GGBFS binders with different nanoparticles (NPs), such as SiO_2, Al_2O_3, Fe_3O_4, and TiO_2 [15,16]. This technique has attracted attention, as it produces notable acceleration effects on the cement hydration process and requires no special arrangements or instruments in construction sites. Promisingly, Sargam and Wang [17] proved that the acceleration impacts of nano-SiO_2, nano-Al_2O_3, and nano-$CaCO_3$ particles were more prominent at low curing temperatures (i.e., 10 °C) when compared to $\geq$ 20 °C. This shows that the employment of NPs can be an easily applicable and efficient solution for enhancing the hardened properties of low-temperature cured cementitious materials in cold regions. More recently, calcium silicate hydrate (C-S-H) seeds with nucleation effects exhibited the highest acceleration impacts on the hydration rate of the silicate and aluminate phases in PC compared to other NPs [18–20]. Wang et al. [19] attributed the superiority of C-S-H seeds to their higher surface area and the lower interfacial energy between seeds and hydration products (i.e., C-S-H) relative to other NPs. With the incorporation of C-S-H seeds, additional nucleation sites and growth templates are being introduced into pore solution for early hydration product precipitation, shortening the induction period, accelerating the hydration rate, increasing the released heat of hydration, and improving the mechanical and durability properties of cementitious materials [12,19,21–23]. Promisingly, Zhang et al. [23] reported that the addition of C-S-H seeds was also efficient in enhancing the strength development of PC-binder cured at −5 °C, with a decreased need for heating systems.

To date, the literature has provided no investigation into the efficiency of C-S-H seeds in boosting the reactivity and strength development of SCMs containing binders cured at very low curing temperatures. To fill this gap, this experimental work aims to decrease the PC content in low-temperature cured binders by increasing the fraction of environmentally and economically friendly GGBFS through the employment of C-S-H seeds. The reactivity, compressive strength development, and frost resistance of 0 °C cured PC/GGBFS binary binders manufactured with GGBFS replacement levels up to 50% and different C-S-H seed contents were investigated and compared to PC-based binder. The hydration process was investigated using isothermal calorimetry, X-ray diffraction (XRD), thermogravimetric/differential thermogravimetry analyses (TGA/DTG), and a selective dissolution test.

2. Materials and experimental methods

Commercially available Portland cement (CEM I 52.5 R) and GGBFS were provided by Finnsementti (Finland). The chemical compositions of PC and GGBFS, as shown in Table 1, were analyzed using X-ray fluorescence (XRF) (PANalytical Omnian Axiosmax). A commercial C-S-H seed admixture (X130-seeds®) was supplied by MBCC (Sweden) with a solid content of ≈23.7% (measured by drying at 105 °C until there was a constant mass). The particle size distributions of PC and GGBFS were measured using a laser diffraction particle size analyzer (LS13320, Beckman coulter, USA), and Malvern Zetasizer Pro (Malvern Instruments, UK) was used for the C-S-H seed size distribution. The median particle sizes (D_{50}) were around 8.5 μm, 9.4 μm, and 0.345 μm for PC, GGBFS, and C-S-H seeds, respectively (Fig. 1). Previously, the authors reported the foil-like amorphous morphology of the C–S–H seeds, as captured via transmission electron microscopy (TEM, JEM-2200FS, Japan) [24]. Detailed seed properties and characterization can be found in the producer-registered patent [25]. A polycarboxylate-based superplasticizer with no retarding effects called Viscocrete-5800 (provided by Sika®, Finland, in compliance with EN 934-2 requirements for water-reducing additives and superplasticizers) with a solid content of ≈35.5% was employed. Deionized water was used in the mixing phase of this study (Section 2.1).

2.1. Binder preparation and curing conditions

Seven binders were developed in this work to investigate the impacts of GGBFS replacement levels (30 and 50 wt% of PC) and C-S-H seed suspension content (2 and 5 wt% of the binder [PC + GGBFS]) on the reactivity and hardened properties of PC/GGBFS binders cured at 0 °C. The adopted dosages of C-S-H seed suspension in this work were based on the previously published work by the authors [24]. The proportions of the mix compositions are provided in Table 2. The water-to-binder (w/b) ratio was kept constant at 0.27 for all

Table 1
Chemical composition of PC and GGBFS.

Material	Oxides (%, w/w)								
	CaO	SiO_2	Al_2O_3	Fe_2O_3	Na_2O	K_2O	MgO	TiO_2	SO_3
PC	69.0	24.0	2.1	0.3	–	–	0.7	–	2.3
GGBFS	38.5	32.3	9.6	1.2	0.5	0.5	10.2	2.2	4.0

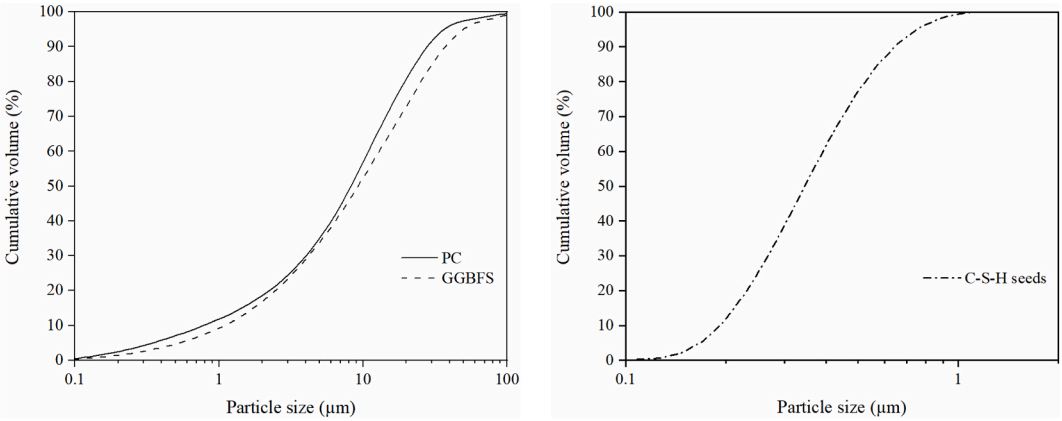

Fig. 1. Particle size distribution of (a) PC and GGBFS, and (b) C-S-H seeds.

binders, taking into account the water content in the superplasticizer and the C-S-H seed suspension. The superplasticizer dosage was optimized using the March cone test and mini-slump test [26,27]. All pastes (with a constant sample volume of 200 mL) have a flow-out time of 30 s through 11 mm nozzle opening. In addition, the flow diameter of the pastes was maintained at 130 mm when truncated cone mold, with height = 35 mm, bottom diameter = 43 mm, and top diameter = 22 mm, was used in the mini-slump test. The decreased dosage of the superplasticizer with the addition of C-S-H seed suspension can be attributed to the presence of nitrate-based dispersing agents [21,25].

First, the dry materials (PC and GGBFS) were mixed for 3 min. The superplasticizer and C-S-H seed solutions were added to the deionized water and kept in an ultrasonic bath (Elmasonic P, Germany) for 5 min [12,28]. The prepared mixing solution was then added to the dry mixed materials and mixed for an additional 3 min. The slurry was cast in 20 × 20 × 20 mm^3 molds, vibrated, and sealed using a plastic sheet to avoid early moisture loss [29]. Thereafter, the pastes in molds were cured in the pre-set freezer at 0 °C for 28 d, representing the average air temperature at the end of autumn season (i.e., November) in Oulu, Finland (65°01′ N, 25°28′ E) (see Fig. A1 in Appendix A). To mimic the frameworks' sides' temperature in construction sites, the molds used in this study were kept in the freezer (0 °C) for one day before casting.

2.2. Analytical methods

The heat release evolution was followed using an isothermal calorimeter (Thermometrics TAM air) to monitor the impacts of the C-S-H seeds and GGBFS replacement levels on the reaction rate of the binders. Since the lowest calorimeter's internal temperature is 5 °C, the heat evolutions of the binders were followed at that temperature, which is higher than the curing temperature of this study. However, the analysis can still provide information about the effects of the seeds and GGBFS on the reactivity of the PC/GGBFS binary binders at low curing temperatures. The calorimeter was set at 5 °C and equilibrated for 1 d. The samples were then prepared according to Section 2.1, and around 5 g of the pastes was poured into glass ampules and kept immediately in the calorimeter. In this study, water was used as a reference sample, and the results were normalized using the pastes' mass.

The impacts of C-S-H seeds on the reaction products evolution and reaction between GGBFS and available calcium hydroxide (i.e., pozzolanic reaction) in the pastes were investigated by thermogravimetric/differential thermogravimetry analyses (TGA/DTG) and XRD analysis. First, the hydration of the samples was stopped by a solvent exchange using isopropanol. The samples were immersed in isopropanol, and the solution was changed twice during the first 2 h [30]. Afterward, the samples were kept in isopropanol for 48 h and then dried in the desiccator at room temperature until the analysis date. The samples were crushed and powdered before testing. The TGA/DTG analysis was performed using an SDT-650 Thermal Analyzer (TA® Instruments, USA). The powder samples (≈15

Table 2
Mix proportions of the study.

	PC (g)	GGBFS (g)	C-S-H seeds solution (g)	SP[(a)] (g)	w/b
S0	100	0	0	0.50	0.27
S30	70	30	0	0.50	
S30–2			2	0.35	
S30–5			5	0.25	
S50	50	50	0	0.50	
S50–2			2	0.35	
S50–5			5	0.25	

(a): Superplasticizer.

mg/sample) were heated from 25 °C to 1000 °C at 10 °C/min in an inert nitrogen atmosphere. The XRD analysis of the specimens was performed using a Rigaku SmartLab diffractometer (Tokyo, Japan) under the following conditions: a voltage of 40 kV, current of 135 mA, step size of 0.02°, scanning speed of 4°2Θ/min, and scanning range of 2Θ = 5°–130°. Phase identification was performed using Rigaku PDXL 2 software with a PDF-4+ 2020 RDB database.

The reactivity of the GGBFS particles was assessed through the ethylene diamine tetra-acetic acid (EDTA)/triethanolamine/NaOH selective dissolution method developed by Luke and Glasser [31]. They showed that unreacted GGBFS particles are acid-insoluble, while hydration products of PC/GGBFS binder and unreacted PC particles are acid-soluble. Therefore, it is possible to dissolve the reaction products of PC/GGBFS binders and unreacted PC particles, leaving the unreacted GGBFS as residue. The detailed test procedures and solvent composition can be found elsewhere [31]. The reacted fractions of GGBFS in the binary binders were calculated using Eq. (1), and the averages of the duplicates were reported for each data point. Corrections were made for anhydrous PC and GGBFS.

$$\text{Reacted GGBFS } (\%) = \left(1 - \frac{\text{insoluble residue of sample} - (\text{CR} \times \text{insoluble residue of anhydrous PC})}{\text{SR} \times \text{insoluble residue of anhydrous GGBFS}}\right) \times 100 \quad (1)$$

where CR: PC mass ratio in the binders and SR: GGBFS mass ratio in the binders.

A compression test was performed using 20 mm^3 cubic paste samples prepared according to Section 2.1. A compression test machine (Z400 Zwick/Roell) with a load cell of 100 kN was used. The average and standard deviation for the six cubes were reported for each data point.

The frost resistance of the paste samples was assessed under rapid freezing and thawing (FT) cycles according to the ASTM C666/C666M − 15 recommendations [32]. Five 28-*d*-old 20 mm^3 cubic samples per mix composition were tested. Samples in plastic containers were placed in a climatic test chamber (WK3-180/40, Weiss Technik, Grand Rapids, USA), and water was added into the containers so that half (≈10 mm) of the samples were submerged in water and the other half were exposed to air. The water level was kept constant throughout the testing period. The samples were subjected to a total of 120 FT cycles with a chamber temperature ranging from −18 °C to +4 °C. One cycle (8 h/cycle) consisted of 2 h at +4 °C, 2h for decreasing the chamber temperature to −18 C, 2 h at −18 °C, and 2 h for increasing the chamber temperature to +4 °C [30]. The visual appearance, mass change (%), and compressive strength of each sample were reported before the test and after the 120 FT cycles.

3. Results and discussion

3.1. Compressive strength development

The compressive strengths of the pastes cured at 0 °C decreased as the GGBFS replacement level increased (Fig. 2). The highest early (i.e., 3 d) compressive strength (≈38 MPa) was measured in the control paste (S0), while the highest (28 d) compressive strength (60.6 MPa) was achieved by the binder containing 30% GGBFS and 2% C-S-H seeds (S30-2). When the GGBFS replacement level was increased to 50 wt%, the lowest 3 d and 28 d compressive strengths of around 18.5 MPa and 40.1 MPa were measured in the S50 pastes, respectively. In this study, the 3 d compressive strengths of S30 and S50 were decreased by around 27.7% and 51.2% compared to the

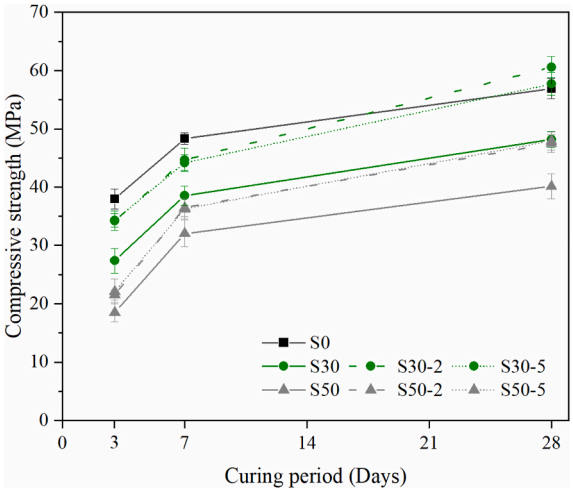

Fig. 2. The impact of GGBFS replacement level and the addition of C-S-H seeds on compressive strength development at 0 °C.

3-*d*-old S0. Over time, the losses in the 28 d compressive strengths of the S30 and S50 pastes were decreased to around 15.4% and 29.5%, respectively, in comparison with the 28-*d*-old S0 (≈57 MPa). This indicates that the side impacts of GGBFS on the compressive strength of the 0 °C cured PC/GGBFS pastes diminished as time passed. The reported reductions in compressive strength with the GGBFS replacement level can be mainly attributed to the lower reaction rate of PC/GGBFS binders at 0 °C relative to S0 because of the lower PC content and slower reaction rate of the GGBFS fraction (as discussed later in Section 3.2). The lower strength loss at a late age than early age can be attributed to the ongoing reaction between GGBFS with liberated calcium hydroxide from the hydration of PC to form additional strength-source C-S-H phase (as shown later in Section 3.3).

According to the results, the compressive strength loss in the PC/GGBFS pastes was diminished by the inclusion of the C-S-H seeds. The C-S-H seed dosage of 2 wt% can be considered the optimal dosage in these conditions, since no further strength enhancements were observed when increasing the seed amount up to 5 wt%, regardless of the curing period. In the presence of 2 wt% C-S-H seeds, the 3 d compressive strength of S30-2 was increased by 24.9% (34.2 MPa) compared with S30 (27.4 MPa), while an increase of around 16.2% (21.5 MPa) was achieved in S50-2 compared to S50 (18.5 MPa). Similar observations were noticed at a late age, where the compressive strengths of 28-*d*-old S30-2 and S50-2 were enhanced by 25.7% (60.6 MPa) and 18.5% (47.5 MPa), respectively, compared to their un-seeded pairs. The latter demonstrates the accelerative impacts of C-S-H seeds on the early and late compressive strength development of PC/GGBFS binders at 0 °C. The findings of this work are consistent with Xu et al. [14] and Zhou et al. [20], who reported enhancements in the strength development of PC/GGBFS and PC/fly ash binders cured at 20 °C in the presence of C-S-H seeds, respectively. Promisingly, the S30-2 binder was able to attain compressive strengths of around 90.2% and 106.5% after 3 d and 28 d curing periods in comparison with those measured in the 3 d and 28-*d*-old S0 pastes, respectively. On the other hand, the 3 d and 28-*d*-old compressive strengths of the S50–2 samples were only 66.1% and 83.5% of those reported in the 3 d and 28 d-old S0 samples, respectively. This shows that the improvements in compressive strength upon the addition of C-S-H seeds were more significant at the low GGBFS replacement level (i.e., 30%) than at the high replacement level (i.e., 50%) in this study. The enhanced compressive strengths of the seeded pastes can be attributed to the nucleation impacts of the C-S-H seeds, which improved the precursors' (i.e., PC and GGBFS) reactivity and the precipitation of strength-source reaction products (as discussed later in Section 3.3).

3.2. Rates of heat evolution and cumulative heat evolved

The hydration heat flow and cumulative released heat of the binders were monitored for 72 h at +5 °C (Fig. 3). Regarding the results, the main peak (i.e., acceleration peak), which is mainly assigned to the hydration of the alite (C_3S) phase in PC, appeared at around 22.6 h (3.2 mW/g) in the control binder (S0). A similar peak was previously reported after 9 h (6.6 mW/g) in type I Portland cement-based binder prepared with a similar w/c ratio of 0.27 at 23 °C [24]. This exhibits the significant decelerative impact of a low curing temperature on the hydration rate of PC-based binders. Furthermore, the appearance of the acceleration peak was further delayed as the GGBFS replacement level increased. Therefore, the acceleration peaks of S30 and S50 were observed 3.5 h and 12.9 h later than S0, respectively. Moreover, the acceleration peak values of S30 and S50 were decreased by 21.9% (2.5 mW/g) and 68.8% (1.0 mW/g) compared to S0. The latter can mainly be attributed to the lower alite content in PC/GGBFS binary binders due to the replacement of PC with GGBFS and to the lower reaction rate of GGBFS at a low curing temperature compared to PC [5,33,34]. A shoulder was also detected in S0 between 30 and 36 h, which is usually attributed to the renewed hydration of tricalcium aluminate (C_3A) and promoted precipitation of ettringite (AFt) [23,33]. This shoulder was previously detected after 16 h in type I Portland cement-based binder prepared with a w/c ratio of 0.3 at 20 °C [23]. Matsushita et al. [35] previously reported that the hydration rate

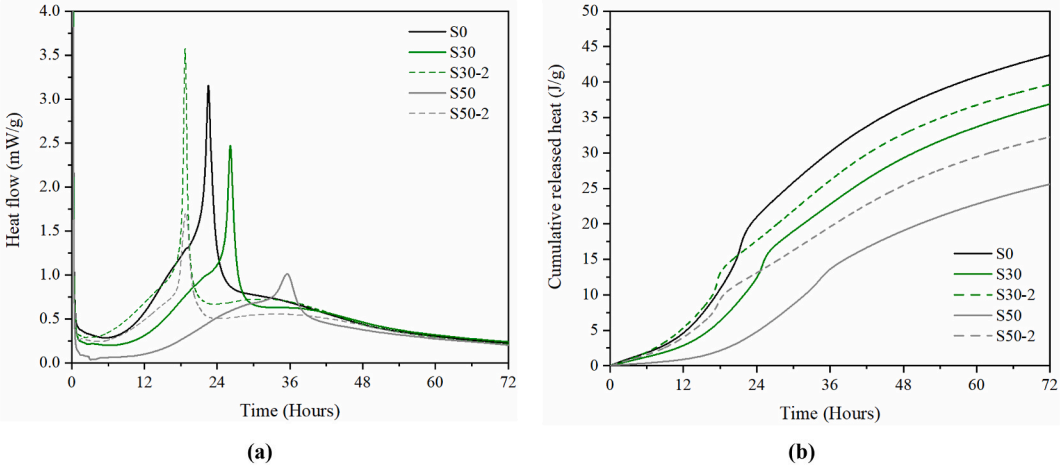

Fig. 3. (a) Heat flow evolution and (b) cumulative heat of hydration of paste samples at +5 °C.

of C_3A and the consumption of gypsum are more negatively affected by low curing temperatures compared to reaction rates in the alite and belite phases. The latter was further confirmed by TGA/DTG results and XRD patterns in Section 3.3.

Regarding the results, the addition of 2 wt% C-S-H seeds significantly shortened the induction period and enhanced the height of the acceleration peaks of the PC/GGBFS binary binders. The acceleration peaks of S30-2 and S50-2 appeared 7.4 h and 16.7 h earlier than those of S30 and S50, respectively. In addition, the acceleration peaks' magnitudes of S30-2 and S50-2 were increased by 44% (3.6 mW/g) and 70% (1.7 mW/g) compared to their un-seeded counterparts, respectively. Interestingly, the seed-modified binary binders exhibited a faster appearance of acceleration peaks when compared to S0, regardless of the GGBFS replacement level. In addition, an increase of around 12.5% in the value of the acceleration peak was achieved in S30-2 in comparison with S0. However, the inclusion of 2% C-S-H was unable to fully compensate for the acceleration peak height drop caused by the 50% GGBFS replacement level in S50-2. Therefore, a reduction of around 40% in the acceleration peak value was calculated in S50-2 compared to S0. Moreover, the shoulder associated with the aluminate phase reaction with gypsum was enhanced in the PC/GGBFS binary binders in the presence of the C-S-H seeds, regardless of the GGBFS content. The latter proves that the reaction of the aluminate phase and the consumption of gypsum were accelerated and enhanced with the addition of the C-S-H seeds. Similar observations were recently reported in seeded PC-based binder [19].

The 72 h cumulative heat (Fig. 3(b)) indicates the hydration degree of the binders [36]. The order of cumulative released heat after 72 h was as follows: S0 (44 J/g) > S30-2 (40 J/g) > S30-0 (37 J/g) > S50-2 (32 J/g) > S50-0 (26 J/g). This shows that the C-S-H seeds enhanced the hydration reaction of the PC/GGBFS binary binders and limited the deceleration impacts of GGBFS on the early reaction rate. The cumulative heat results are in good agreement with compressive strength measurements (Section 3.1) and the amounts of precipitated reaction products, as will be shown later in the TGA/DTG results (Section 3.3).

The accelerated hydration process of the seeded PC/GGBFS binders can be attributed to the nucleation effects of the added C-S-H seeds [14,19]. The dissolution-precipitation theory suggests that the induction period during the hydration process of cementitious materials is mainly affected by the formation of stable nuclei for the following rapid hydration product precipitation during the acceleration period [22]. In addition, Wang et al. [19] showed that the total growing surface area for hydration product precipitation and growth is defined by the number of nuclei formed during the induction period in PC-based binding systems. Therefore, the accelerated and enhanced availability of dispersed nucleation sites and increased total growing surface area in the pore solutions of the seeded binary binders because of the inclusion of the C-S-H seeds illustrates the boosted and enhanced reactivity of the seeded binders. In

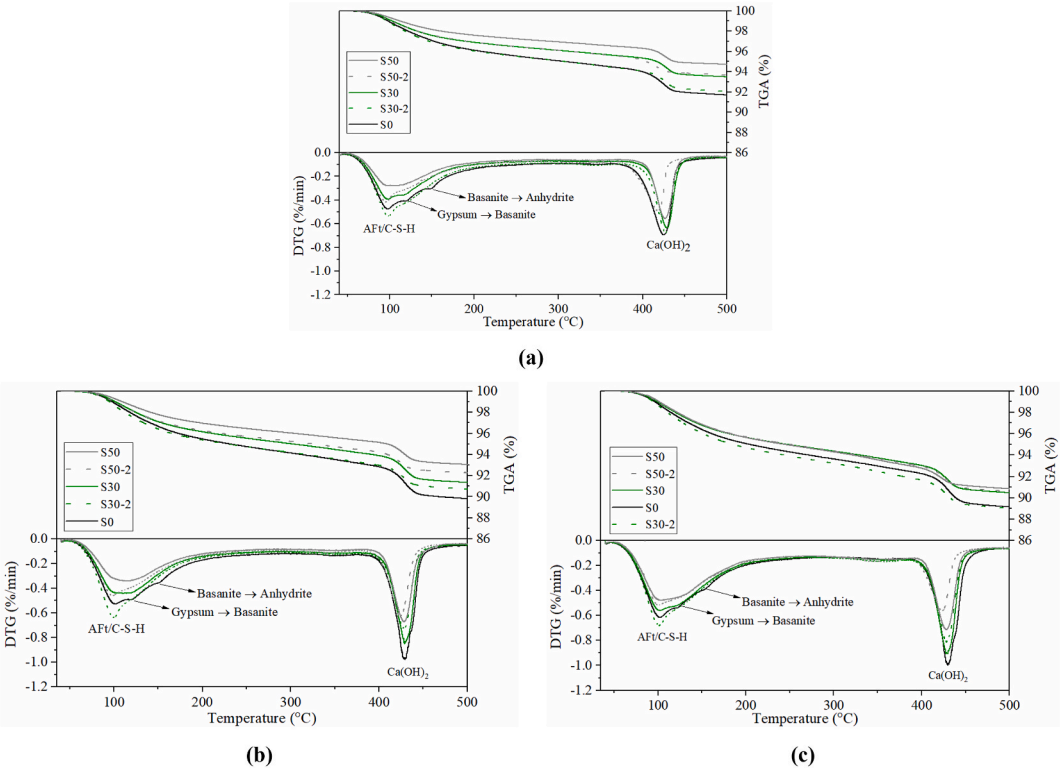

Fig. 4. TGA/DTG curves of (a) 3 d, (b) 7 d, (c) 28-*d*-old binders.

addition, the presence of additional stable C-S-H nuclei at an early age favors gel precipitation over dispersed C-S-H nuclei and away from the surfaces of the precursors' (i.e., PC and GGBFS) particles [17,19,21–23]. This shifted gel precipitation location limits the early formation of a semi-impermeable hydrate layer over anhydrous precursor particles, thereby enhancing the subsequent dissolution process of the precursors and accelerating the follow-up hydration reaction [37,38].

3.3. Hydration evolution and products

The precipitated gel content decreased with increasing GGBFS replacement levels and increased with curing time and the addition of C-S-H seeds (Fig. 4). Regarding the DTG curves, the first peak was identified between 60 and 115 °C, which is associated with the decomposition of the ettringite (AFt) phase and dehydration of the C-S-H reaction product [39]. The dehydration of residual gypsum ($CaSO_4{\cdot}2H_2O$) involved an initial loss of 75% of the water molecules and thereby formed basanite ($Ca_2SO_4{\cdot}0.5H_2O$) between 115 and 125 °C, followed by complete dehydration to anhydrite at 140–160 °C [40]. The endotherms at 380–450 °C are a result of the dehydroxylation of $Ca(OH)_2$ [41,42].

The TGA/DTG results showed that the unseeded S30 and S50 binders provided lower AFt and C-S-H contents compared to S0, regardless of the curing period. This is mainly attributable to the lower PC fraction in the binary binders and the lower reaction rate of GGBFS at 0 °C relative to PC [5]. Nevertheless, the addition of the C-S-H seeds accelerated the reaction rate of the PC/GGBFS binders, and higher amounts of AFt and C-S-H were formed in the S30-2 and S50-2 binders when compared to their unseeded counterparts, regardless of the curing period. Promisingly, S30-2 exhibited higher AFt and C-S-H amounts compared to S0, regardless of the curing period. This proves that the inclusion of C-S-H seeds diminished the side impacts of GGBFS on the content of developed reaction products at 0 °C by accelerating the hydration of the PC fraction and thus fully compensating for the reduced AFt and C-S-H amounts caused by the 30% GGBFS replacement level. However, when the GGBSF replacement level was leveled up to 50% in the seed-modified S50-2 binder, lower AFt and C-S-H contents were measured in comparison with S0, regardless of the curing time. The enhanced early (i.e., 3 d) hydration products' precipitation in the seeded binary binders was consistent with the isothermal calorimeter measurements (see Fig. 3 in Section 3.2). Furthermore, the XRD analysis showed that the reactivity and consumption of the silicate phases and gypsum were enhanced in the presence of the C-S-H seeds in the 28-*d*-old PC/GGBFS binders (Fig. 5). The latter illustrates the higher contents of the precipitated C-S-H and AFt reaction products in the 28 d-old seeded samples relative to the unseeded samples (Fig. 4 (c)). The accelerated and enhanced gel precipitation in the seeded binary binders can mainly be assigned to the nucleation effects of C-S-H seeds, as discussed earlier in Section 3.2. Similar enhancements in gel content were recently reported in C-S-H seed-modified PC [21,23], PC/GGBFS [14], and PC/fly ash [20] binders cured at 20–25 °C.

When considering the residual gypsum dehydration peaks (Fig. 4), it was observed that their intensities were continuously, but slowly, decreased with time due to the ongoing reaction between the alumina phases and gypsum, which forms ettringite. The lower gypsum dehydration peak intensity in the binary binders can be attributed to the lower total gypsum content, which is due to the partial replacement of PC by GGBFS. Furthermore, the intensities of the gypsum dehydration peaks in the binary binders were reduced in the presence of the C-S-H seeds. This can be attributed to the accelerated reaction between alumina phases and gypsum in the

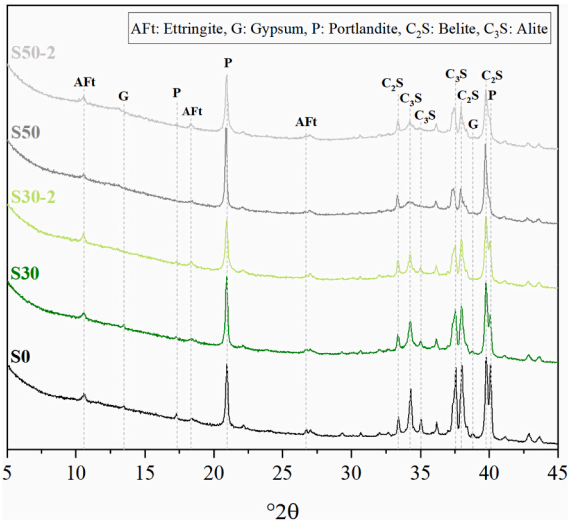

Fig. 5. XRD patterns of the selected 28-*d*-old binders.

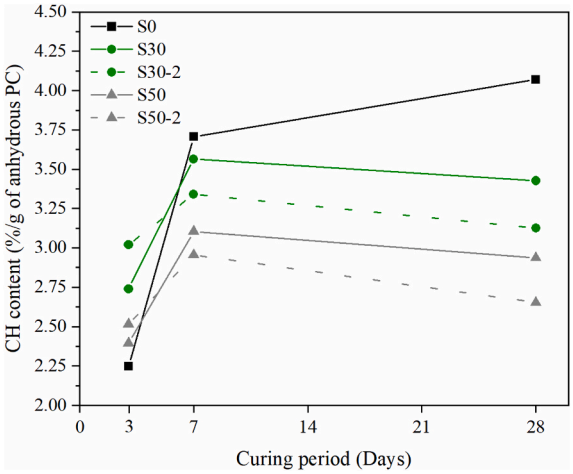

Fig. 6. Change in CH content with time, GGBFS replacement level, and addition of C-S-H seeds.

presence of C-S-H seeds, which was demonstrated earlier in Section 3.2. Therefore, the gypsum dehydration peaks disappeared in the seeded PC/GGBFS binary binders (i.e., S30-2 and SS50-2) from 7 d onwards, while they were still detectable in the S0 and unseeded blends, even at 28 d. The XRD results of 28-*d*-old samples confirm these observations (Fig. 5).

3.3.1. CH content

The calcium hydroxide (CH, $Ca(OH)_2$) contents (Fig. 6) were calculated using TGA mass loss curves (from Fig. 4) and a graphical technique [43,44]. The CH contents were calculated by the mass of anhydrous PC present in the ignited samples considering the loss of ignition (LOI) of the PC and GGBFS fractions. Expressing the CH content per unit mass of anhydrous PC, and not the total mass of ignited samples, permits a better estimation of the starting time and extent of pozzolanic reaction in the binary binders.

Fig. 6 shows that the CH content in the reference binder (S0) was increased over time up to 28 d, reaching a maximum of ≈4.1%. However, the CH contents in the 3 d and 28 d-old S0 binder were ≈78.6% and 67.4% lower than those reported in PC-based binder prepared with w/c of 0.3 and cured at 27 °C [45]. The latter shows the significant decelerative impact of low curing temperature (i.e., 0 °C) on the early and late hydration progress. It is known that the CH content in a PC-based binder indicates the hydration degree of PC. In addition, it was noticed that the detrimental impacts of 0 °C on the hydration degree of PC-based binder were slightly diminished with time when compared to that cured at 27 °C. Similarly, Yang et al. [46] reported a lower loss in the hydration degree of PC-based binder cured at 5 °C with time, when compared to that cured at 20 °C.

Regarding the binary binders, the total amount of CH depends on the PC hydration that produces CH and the pozzolanic reaction of GGBFS that consumes CH. According to the results, the production of CH was a dominant process at an early age, and the pozzolanic reaction of GGBFS was then started consuming the available CH. Therefore, the CH amounts were initially increased during the first seven days of the curing period, and thereafter, CH contents started to decrease in the binary binders. At 3 d, higher CH contents (%/g of anhydrous PC) were measured in all PC/GGBFS binary binders in comparison with S0. Due to the low early hydration rate of GGBFS, the water-to-PC ratios in the binary binders were indirectly higher than those of S0 as a result of the lower water consumption by GGBFS [47,48]. Previously, Feldman [49] and Wang [44] proved that increasing the water-to-PC ratio is beneficial for the PC hydration process, enhancing the degree of hydration and increasing the CH content. Moreover, the higher CH contents in the 3-*d*-old seeded binary binders, compared to their unseeded pairs, can be attributed to the acceleration impacts of C-S-H seeds on the reactivity of the PC fraction as a result of the nucleation effects of the seeds (as discussed earlier in Section 3.2). Furthermore, increases in the CH contents were observed in 7-*d*-old PC/GGBFS binders compared to their 3-*d*-old pairs. The increased CH content in the binary binders during the first seven days of the curing period indicates that the rate of CH liberation through the PC hydration process is faster and higher than the CH consumption rate through the pozzolanic reaction of GGBFS at 0 °C. Soutsos et al. [5] and Yang et al. [46] demonstrated that the reactivity of PC is significantly faster than that of GGBFS at low curing temperatures (i.e., 10 °C and 5 °C, respectively). However, from 7 d onwards, all PC/GGBFS binders showed lower CH contents than S0, regardless of the GGBFS replacement level and C-S-H seed addition, which can be attributed to the consumption of available CH by active silica from GGBFS to produce additional C-S-H phase [50–54]. Promisingly, it was observed that the pozzolanic reaction rate of GGBFS was enhanced with the addition of C-S-H seeds and the curing period. When compared with the CH in the S0 binder, higher CH consumption was observed in the seeded binary binders than in their unseeded counterparts. The enhanced reactivity GGBFS in the presence of C-S-H seeds

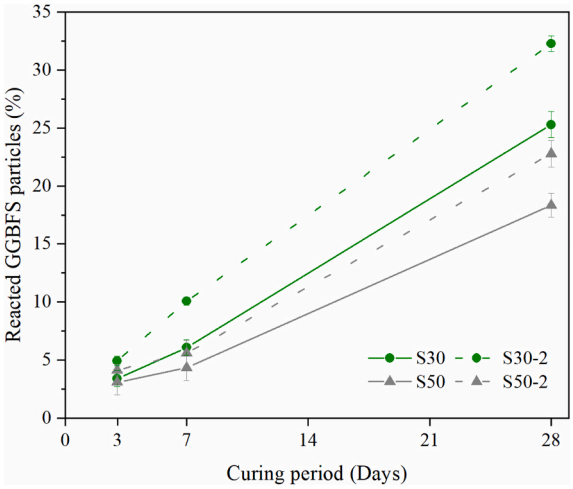

Fig. 7. The influence of C-S-H seeds on the reactivity of GGBFS in binary PC/GGBFS binders.

illustrates the enhanced compressive strength development in the seeded samples (see Fig. 2 in Section 3.1).

3.3.2. *GGBFS reaction assessment*

Several studies have previously demonstrated the enhanced reactivity of PC-based binder in the presence of C-S-H seeds, showing that it results in a lower fraction of unreacted cement particles compared to its unseeded counterpart [12,17,21–23]. In this study, a selective dissolution test was performed to explore the impacts of the C-S-H seeds on the reactivity of the GGBFS fraction in the binary PC/GGBFS binder at 0 °C. The latter helps pose the question as to whether the enhanced mechanical properties (Section 3.1), accelerated reaction rates (Section 3.2), and improved reaction product formation (Section 3.3) of the seeded binders are only assigned to the enhanced reactivity of PC due to the addition of C-S-H seeds, or whether the pozzolanic reaction degree of GGBFS was also improved.

Fig. 7 shows that the amounts of reacted GGBFS were increased with time and the addition of C-S-H seeds, indicating the enhanced reaction between GGBFS and available CH. In addition, the selective dissolution results showed that the degree of pozzolanic reaction of GGBFS was higher (i.e., there were more reacted GGBFS particles) at a replacement level of 30% than at 50%. Similarly, Esfahani et al. [55] showed that increasing the GGBFS content in PC/GGBFS concrete reduced the amount of reacted GGBFS particles. The higher reaction degree of GGBFS in PC/GGBFS binders with a lower replacement level (i.e., 30%) can be attributed to the higher availability of CH for GGBFS to react with (see Fig. 6). Saeki and Monteiro [56] proved that the degree of pozzolanic reaction of GGBFS is dependent on the amount of available CH.

According to the results, limited GGBFS particles (<5%) were reacted in the 3-*d*-old PC/GGBFS binders, regardless of the GGBFS replacement level and the addition of C-S-H seeds. The latter confirms the low early reactivity of GGBFS at 0 °C, even in the presence of C-S-H seeds. This observation is in line with the early CH consumption rate (see Fig. 6 in Section 3.3.1). At 7 and 28 d, the amount of reacted GGBFS particles in the seeded S30-2 binder were 10.1% and 32.3%, which were 65.6% and 27.7% higher than those measured in the unseeded S30 binder. Similarly, the 7 d and 28-*d*-old S50-2 binder achieved 30.2% and 24.4% higher reacted amounts of GGBFS compared to S50. The results of the selective dissolution test indicate that the observed early (i.e., 3 d) strength enhancements (Fig. 2), accelerated reaction rates, and gel precipitation (Figs. 3 and 4) in the seeded binders are mainly attributable to the acceleration impacts of C-S-H seeds on PC hydration, while the pozzolanic reaction of GGBFS with available CH participated in the precipitation of additional strength-source reaction products (i.e., C-S-H, see Fig. 4) which enhanced the compressive strength of binary pastes from 7 d onwards.

The enhanced reaction degree of GGBFS in the presence of C-S-H seeds can be attributed to the nucleation effect of C-S-H seeds and the increased alkalinity of pore solution. With the addition of the seeds, the dissolution and reactivity of the PC fraction were enhanced owing to the nucleation effects of the seeds (see Figs. 3 and 5), increasing the amount of precipitated CH in the seeded binders (see Fig. 6) and thereby increasing the alkalinity of the pore solution [23,42,57,58]. In addition, Ersoy et al. [59] and Hewlett and Lisk [60] demonstrated the increased pH of pore solution with the enhanced dissolution of PC clinker due to the increased number of released hydroxide ions. Because of the enhanced alkalinity of pore solution, the dissolution of GGBFS grains and reaction between GGBFS and CH were accelerated and enhanced in the seeded binders.

3.4. Frost resistance

Regarding the visual appearance of the samples, no surface cracks or spalling (i.e., scaling) were observed in the S0, S30-2, and S30-5 samples after 120 freeze-thaw (FT) cycles (Fig. 8). However, in the absence of C-S-H seeds, S30 exhibited low frost resistance, and as a result, surface cracks and spalling were detected. In addition, when the GGBFS replacement leveled up to 50%, the samples were entirely damaged, regardless of the C-S-H seed content. The mass losses of surviving samples (i.e., S0, S30-2, and S30-5) were calculated, and averages of around 2.7%, 0.5%, and 1.0% were registered, respectively. In line with the mass losses, around 53%, 30%, and 33% compressive strength reductions were measured after 120 FT cycles in S0, S30-2, and S30-5, respectively (Fig. 9). The higher frost resistance of the S30-2 and S30-5 binders compared to the S0 binder can be attributed to the improved PC hydration process and increased amount of reacted GGBFS in the presence of C-S-H seeds (see Figs. 4 and 7) and to the micro-filling ability of GGBFS [55,61]. The latter densified the microstructures of the seeded S30-2 and S30-5 samples, hence limiting the water ingress into their microstructure and reducing the microstructural damage caused by the increased internal hydraulic stress exerted by the volume expansion of ice formed in the pore structures [57,62]. On the other hand, the decreased frost resistances of S30, S50, S50-2, and S50-5 can be attributed to their low reactivity at 0 °C (see Fig. 4) and high amounts of unreacted GGBFS particles (Fig. 7), which degrade the quality of the microstructure [55]. Therefore, their microstructures were incapable of withstanding the expansion hydraulic stress of the frozen pore solution. Similarly, Tavasoli et al. [62] and Amran et al. [10] reported a decrease in frost resistance, with increasing GGBFS replacement in the PC/GGBFS binary binders cured at room temperature.

The results of the FT resistance assessment show that the mutual use of GGBFS and C-S-H seeds can enhance the frost resistance of low-temperature cured binary binders. Therefore, the addition of C-S-H seeds can be considered an efficient method to increase the utilization of GGBFS in cold weather-cured cementitious binders while maintaining or even enhancing their durability properties.

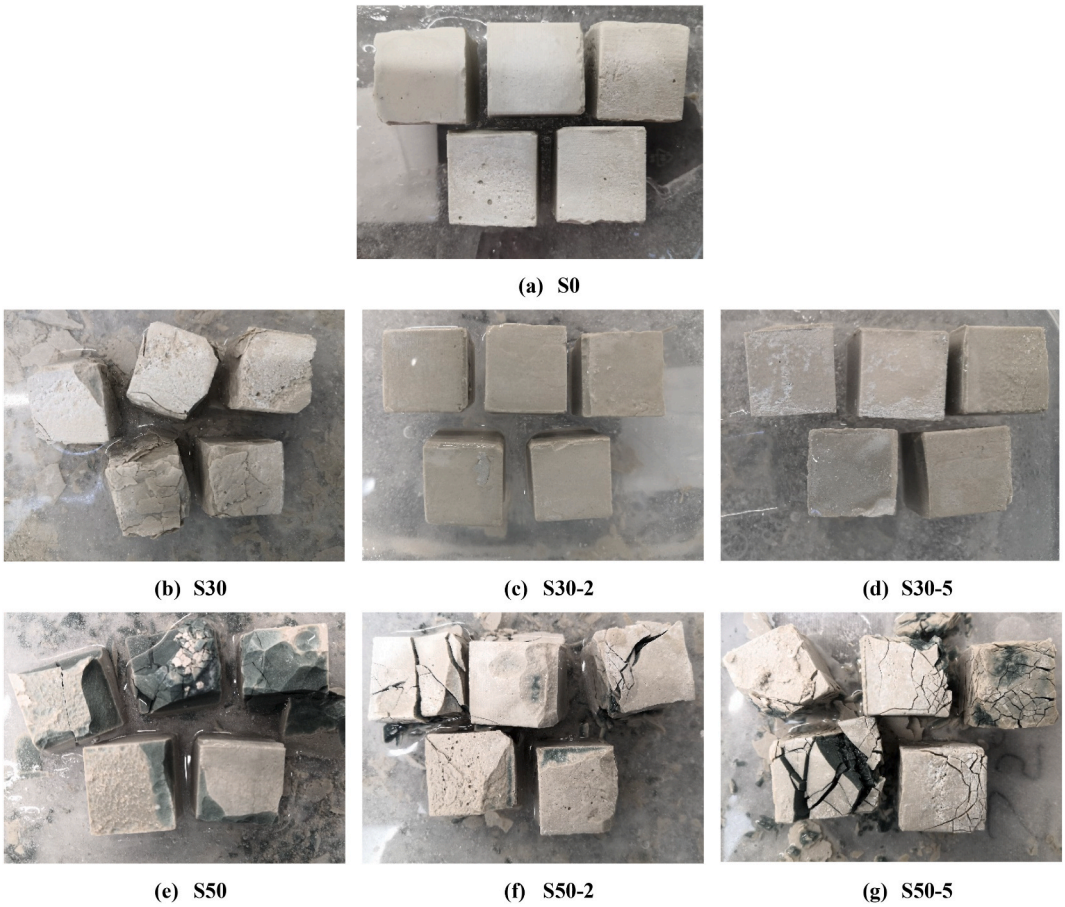

Fig. 8. The visual appearance of the 20 cm^3 cubic paste samples after 120 freeze-thaw cycles.
(a) S0
(b) S30 (c) S30-2 (d) S30-5
(e) S50 (f) S50-2 (g) S50-5

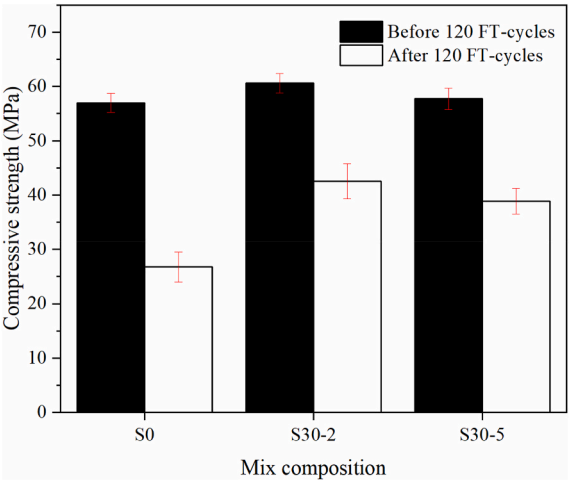

Fig. 9. Impacts of 120 freeze-thaw cycles on compressive strength.

4. Conclusion

This work aims to enhance the sustainability of winter construction works in cold regions by increasing the utilization of GGBFS in cold weather concreting. The study investigates the impacts of C-S-H seeds on the reactivity, strength development, durability properties, and cost- and eco-performance of 0 °C cured Portland cement (PC)/ground granulated blast furnace slag (GGBFS) binary binders prepared with different GGBFS replacement levels (30% and 50%) and C-S-H seed dosages (2% and 5%).

Replacing PC with GGBFS reduces the compressive strength of 0 °C cured binders. The strength loss in the binary binder is more obvious at an early age (i.e., 3 d) and a high GGBFS replacement level (50%). The addition of C-S-H seeds increases the compressive strength of the binary binder, regardless of the GGBFS replacement level and curing period. In the presence of the optimal dosage (i.e., 2%) of C-S-H seeds, the 3 d and 28-*d*-old 70%PC/30%GGBFS and 50%PC/50%GGBFS binders gained 24.9% and 16.2%, and 25.7% and 18.5% higher compressive strengths than their unseeded pairs, respectively. Promisingly, the 70%PC/30%GGBFS binder modified with 2% C-S-H seeds can achieve 3 d and 28 d compressive strengths of around 90.2% and 106.5% of those measured in the PC-based binder, respectively. The heat of hydration measurement shows that the C-S-H seeds accelerate and enhance the reaction rate of the binary binders, regardless of the GGBFS replacement level. The inclusion of the C-S-H seeds increases the amount of precipitated C-S-H and ettringite responsible for binder strength. The presence of C-S-H seeds improves the pozzolanic reaction between GGBFS and available calcium hydroxide liberated from the hydration of PC from 7 d onwards, increasing the amount of reacted GGBFS and the consumption of calcium hydroxide. The seeds-modified 70%PC/30%GGBFS binder can gain better frost resistance than the PC binder. The findings of this experimental work show the real potential of increasing the share of GGBFS in cold weather construction works through the nucleation and seeding technologies provided by C-S-H seeds.

Author contributions

Ahmad Alzaza: Conceptualization, Data curation, Formal analysis, Investigation, Methodology, Validation, Visualization, Writing—original draft, Writing—review & editing. **Katja Ohenoja**: Conceptualization, Methodology, Formal analysis, Validation, Visualization, Writing—review & editing, Supervision, Funding acquisition. Mirja Illikainen: Conceptualization, Resources, Visualization, Writing—review & editing, Supervision, Funding acquisition.

Funding

This work was carried out under the auspices of the ARCTIC-ecocrete project, which is supported by the Interreg Nord program. This program is funded by the European Regional Development Fund and the Regional Council of Lapland.

Declaration of competing interest

The authors declare that they have no known competing financial interests or personal relationships that could have appeared to influence the work reported in this paper.

Acknowledgments

Mr. Jarno Karvonen and Mr. Tun Nyo are acknowledged for their contributions to the laboratory work. Mr. Håkan Nykvist (Master Builders Solutions, Sweden), Mr. Petri Manninen (Sika, Finland), and Mr. Esa Heikkilä (Finnsementti, Finland) are acknowledged for providing materials for this study. The authors thank the Centre for Material Analysis, University of Oulu, Finland.

Appendix A

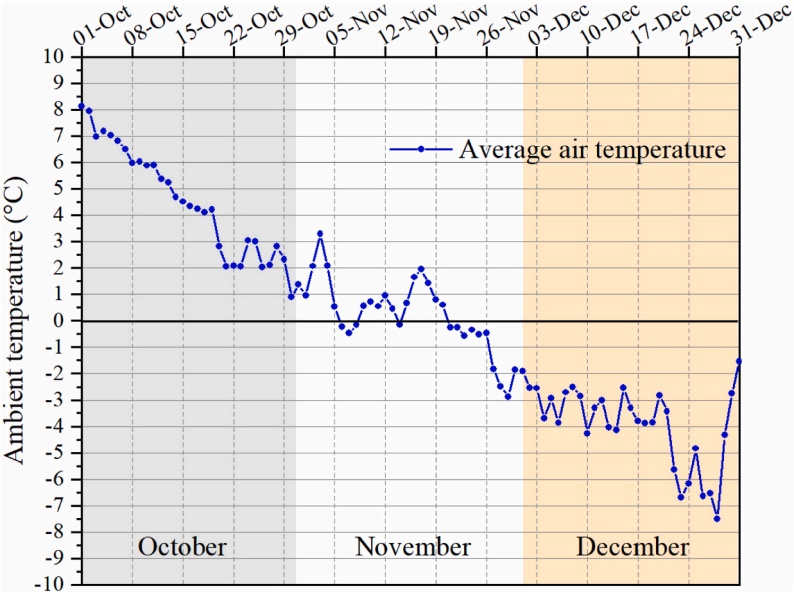

Fig. A1. Average air temperature (2010–2020) in Oulu, Finland (65°01′ N, 25°28′ E) [63].

References

[1] ACI Committee, Guide to Cold Weather Concreting "ACI 306R-10, " Am. Concr. Inst. Farmington Hills Mich. USA, 2010.

[2] J. Dai, Q. Wang, X. Lou, X. Bao, B. Zhang, J. Wang, X. Zhang, Solution calorimetry to assess effects of water-cement ratio and low temperature on hydration heat of cement, Construct. Build. Mater. 269 (2021), 121222, https://doi.org/10.1016/j.conbuildmat.2020.121222.

[3] H. Zhao, K. Jiang, Y. Di, W. Xu, W. Li, Q. Tian, J. Liu, Effects of curing temperature and superabsorbent polymers on hydration of early-age cement paste containing a CaO-based expansive additive, Mater. Struct. 52 (2019) 108, https://doi.org/10.1617/s11527-019-1407-0.

[4] C.K. Nmai, Cold weather concreting admixtures, Cement Concr. Compos. 20 (1998) 121–128, https://doi.org/10.1016/S0958-9465(97)00063-2.

[5] M. Soutsos, A. Hatzitheodorou, F. Kanavaris, J. Kwasny, Effect of temperature on the strength development of mortar mixes with GGBS and fly ash, Mag. Concr. Res. 69 (2017) 787–801, https://doi.org/10.1680/jmacr.16.00268.

[6] C. Meyer, The greening of the concrete industry, Cement Concr. Compos. 31 (2009) 601–605, https://doi.org/10.1016/j.cemconcomp.2008.12.010.

[7] J.X. Peng, L. Huang, Y.B. Zhao, P. Chen, L. Zeng, W. Zheng, Modeling of carbon dioxide measurement on cement plants, Adv. Mater. Res. 610–613 (2013) 2120–2128. www.scientific.net/AMR.610-613.2120.

[8] S.A. Miller, Supplementary cementitious materials to mitigate greenhouse gas emissions from concrete: can there be too much of a good thing? J. Clean. Prod. 178 (2018) 587–598, https://doi.org/10.1016/j.jclepro.2018.01.008.

[9] J. Sun, P. Zhang, Effects of different composite mineral admixtures on the early hydration and long-term properties of cement-based materials: a comparative study, Construct. Build. Mater. 294 (2021), 123547, https://doi.org/10.1016/j.conbuildmat.2021.123547.

[10] M. Amran, G. Murali, N.H.A. Khalid, R. Fediuk, T. Ozbakkaloglu, Y.H. Lee, S. Haruna, Y.Y. Lee, Slag uses in making an ecofriendly and sustainable concrete: a review, Construct. Build. Mater. 272 (2021), 121942, https://doi.org/10.1016/j.conbuildmat.2020.121942.

[11] M.M.A. Elahi, C.R. Shearer, A. Naser Rashid Reza, A.K. Saha, M.N.N. Khan, M.M. Hossain, P.K. Sarker, Improving the sulfate attack resistance of concrete by using supplementary cementitious materials (SCMs): a review, Construct. Build. Mater. 281 (2021), 122628, https://doi.org/10.1016/j.conbuildmat.2021.122628.

[12] J. Li, W. Zhang, K. Xu, P.J.M. Monteiro, Fibrillar calcium silicate hydrate seeds from hydrated tricalcium silicate lower cement demand, Cement Concr. Res. 137 (2020), 106195, https://doi.org/10.1016/j.cemconres.2020.106195.

[13] M. Saillio, V. Baroghel-Bouny, S. Pradelle, M. Bertin, J. Vincent, J.-B. d'Espinose de Lacaillerie, Effect of supplementary cementitious materials on carbonation of cement pastes, Cement Concr. Res. 142 (2021), 106358, https://doi.org/10.1016/j.cemconres.2021.106358.

[14] C. Xu, H. Li, X. Yang, Effect and characterization of the nucleation C-S-H seed on the reactivity of granulated blast furnace slag powder, Construct. Build. Mater. 238 (2020), 117726, https://doi.org/10.1016/j.conbuildmat.2019.117726.

[15] M.S. Amin, S.M.A. El-Gamal, F.S. Hashem, Effect of addition of nano-magnetite on the hydration characteristics of hardened Portland cement and high slag cement pastes, J. Therm. Anal. Calorim. 112 (2013) 1253–1259, https://doi.org/10.1007/s10973-012-2663-1.

[16] A. Nazari, S. Riahi, The role of SiO2 nanoparticles and ground granulated blast furnace slag admixtures on physical, thermal and mechanical properties of self compacting concrete, Mater. Sci. Eng. 528 (2011) 2149–2157, https://doi.org/10.1016/j.msea.2010.11.064.

[17] Y. Sargam, K. Wang, Hydration kinetics and activation energy of cement pastes containing various nanoparticles, Compos. B Eng. 216 (2021), 108836, https://doi.org/10.1016/j.compositesb.2021.108836.

[18] G. Land, D. Stephan, Controlling cement hydration with nanoparticles, Cement Concr. Compos. 57 (2015) 64–67, https://doi.org/10.1016/j.cemconcomp.2014.12.003.

[19] F. Wang, X. Kong, D. Wang, Q. Wang, The effects of nano-C-S-H with different polymer stabilizers on early cement hydration, J. Am. Ceram. Soc. 102 (2019) 5103–5116, https://doi.org/10.1111/jace.16425.

[20] Z. Zhou, M. Sofi, J. Liu, S. Li, A. Zhong, P. Mendis, Nano-CSH modified high volume fly ash concrete: early-age properties and environmental impact analysis, J. Clean. Prod. 286 (2021), 124924, https://doi.org/10.1016/j.jclepro.2020.124924.

[21] H.C. Pedrosa, O.M. Reales, V.D. Reis, M. das D. Paiva, E.M.R. Fairbairn, Hydration of Portland cement accelerated by C-S-H seeds at different temperatures, Cement Concr. Res. 129 (2020), 105978, https://doi.org/10.1016/j.cemconres.2020.105978.

[22] F. Wang, X. Kong, L. Jiang, D. Wang, The acceleration mechanism of nano-C-S-H particles on OPC hydration, Construct. Build. Mater. 249 (2020), 118734, https://doi.org/10.1016/j.conbuildmat.2020.118734.

[23] G. Zhang, Y. Yang, H. Li, Calcium-silicate-hydrate seeds as an accelerator for saving energy in cold weather concreting, Construct. Build. Mater. 264 (2020), 120191, https://doi.org/10.1016/j.conbuildmat.2020.120191.

[24] A. Alzaza, K. Ohenoja, I. Langås, B. Arntsen, M. Poikelispää, M. Illikainen, Low-temperature (−10 °C) curing of Portland cement paste – synergetic effects of chloride-free antifreeze admixture, C–S–H seeds, and room-temperature pre-curing, Cement Concr. Compos. 125 (2022), 104319, https://doi.org/10.1016/j.cemconcomp.2021.104319.

[25] L. Nicoleau, G. Albrecht, K. Lorenz, E. Jetzlsperger, D. Fridrich, T. Wohlhaupter, R. Dorfner, H. Leitner, M. Vierle, D. Schmitt, M. Braeu, C. Hesse, S.M. Pancera, S. Zuern, M. Kutschera, Plasticizer-containing Hardening Accelerator Composition, US8653186B2, 2014. https://patents.google.com/patent/US8653186B2/en. (Accessed 1 April 2021).

[26] L. Agulló, B. Toralles-Carbonari, R. Gettu, A. Aguado, Fluidity of cement pastes with mineral admixtures and superplasticizer—a study based on the Marsh cone test, Mater. Struct. 32 (1999) 479–485, https://doi.org/10.1007/BF02481631.

[27] D.L. Kantro, Influence of water-reducing admixtures on properties of cement paste—a miniature slump test, Cem. Concr. Aggregates 2 (1980) 95–102.

[28] K. Behfarnia, M. Rostami, Effects of micro and nanoparticles of SiO2 on the permeability of alkali activated slag concrete, Construct. Build. Mater. 131 (2017) 205–213, https://doi.org/10.1016/j.conbuildmat.2016.11.070.

[29] A. Alzaza, K. Ohenoja, M. Illikainen, One-part alkali-activated blast furnace slag for sustainable construction at subzero temperatures, Construct. Build. Mater. 276 (2021), 122026, https://doi.org/10.1016/j.conbuildmat.2020.122026.

[30] A. Alzaza, K. Ohenoja, M. Illikainen, Enhancing the mechanical and durability properties of subzero-cured one-part alkali-activated blast furnace slag mortar by using submicron metallurgical residue as an additive, Cement Concr. Compos. (2021), 104128, https://doi.org/10.1016/j.cemconcomp.2021.104128.

[31] K. Luke, F.P. Glasser, Selective dissolution of hydrated blast furnace slag cements, Cement Concr. Res. 17 (1987) 273–282, https://doi.org/10.1016/0008-8846(87)90110-4.

[32] ASTM C666/C666M–15, Standard Test Method for Resistance of Concrete to Rapid Freezing and Thawing, ASTM International, West Conshohocken, PA, USA, 2015. www.astm.org.

[33] J.I. Escalante-Garcia, J.H. Sharp, The effect of temperature on the early hydration of Portland cement and blended cements, Adv. Cement Res. 12 (2000) 121–130, https://doi.org/10.1680/adcr.2000.12.3.121.

[34] H.-M. Woo, C.-Y. Kim, J.H. Yeon, Heat of hydration and mechanical properties of mass concrete with high-volume GGBFS replacements, J. Therm. Anal. Calorim. 132 (2018) 599–609, https://doi.org/10.1007/s10973-017-6914-z.

[35] T. Matsushita, S. Hoshino, I. Maruyama, T. Noguchi, K. Yamada, Effect of curing temperature and water to cement ratio on hydration of cement compounds, in: Proceedings of 12th International Congress on the Chemistry of Cement, Montreal, 2007.

[36] H.F.W. Taylor, Cement Chemistry, second ed., T. Telford, London, 1997.

[37] S. Rahimi-Aghdam, Z.P. Bažant, M.J. Abdolhosseini Qomi, Cement hydration from hours to centuries controlled by diffusion through barrier shells of C-S-H, J. Mech. Phys. Solid. 99 (2017) 211–224, https://doi.org/10.1016/j.jmps.2016.10.010.

[38] S. Bishnoi, K.L. Scrivener, Studying nucleation and growth kinetics of alite hydration using μic, Cement Concr. Res. 39 (2009) 849–860, https://doi.org/10.1016/j.cemconres.2009.07.004.

[39] H. Song, Y. Jeong, S. Bae, Y. Jun, S. Yoon, J. Eun Oh, A study of thermal decomposition of phases in cementitious systems using HT-XRD and TG, Construct. Build. Mater. 169 (2018) 648–661, https://doi.org/10.1016/j.conbuildmat.2018.03.001.

[40] A.J. Pinto, A. Jimenez, M. Prieto, Dehydration behaviour of the Ca(SO_4,HPO_4).2H_2O solid solution, Mineral. Mag. 72 (2008) 277–281, https://doi.org/10.1180/minmag.2008.072.1.277.

[41] D. Jansen, Ch Naber, D. Ectors, Z. Lu, X.-M. Kong, F. Goetz-Neunhoeffer, J. Neubauer, The early hydration of OPC investigated by in-situ XRD, heat flow calorimetry, pore water analysis and 1H NMR: learning about adsorbed ions from a complete mass balance approach, Cement Concr. Res. 109 (2018) 230–242, https://doi.org/10.1016/j.cemconres.2018.04.017.

[42] P. Shafigh, S. Yousuf, J.C. Lee, Z. Ibrahim, The effect of cement mortar composition on the pH value, IOP Conf. Ser. Mater. Sci. Eng. 770 (2020), 012026, https://doi.org/10.1088/1757-899X/770/1/012026.

[43] B.K. Marsh, R.L. Day, Pozzolanic and cementitious reactions of fly ash in blended cement pastes, Cement Concr. Res. 18 (1988) 301–310, https://doi.org/10.1016/0008-8846(88)90014-2.

[44] X.-Y. Wang, Properties prediction of ultra high performance concrete using blended cement hydration model, Construct. Build. Mater. 64 (2014) 1–10, https://doi.org/10.1016/j.conbuildmat.2014.04.084.

[45] C.-S. Poon, L. Lam, S.C. Kou, Y.-L. Wong, R. Wong, Rate of pozzolanic reaction of metakaolin in high-performance cement pastes, Cement Concr. Res. 31 (2001) 1301–1306, https://doi.org/10.1016/S0008-8846(01)00581-6.

[46] H.-M. Yang, S.-J. Kwon, N.V. Myung, J.K. Singh, H.-S. Lee, S. Mandal, Evaluation of strength development in concrete with ground granulated blast furnace slag using apparent activation energy, Materials 13 (2020) 442, https://doi.org/10.3390/ma13020442.

[47] B. Kolani, L. Buffo-Lacarrière, A. Sellier, G. Escadeillas, L. Boutillon, L. Linger, Hydration of slag-blended cements, Cement Concr. Compos. 34 (2012) 1009–1018, https://doi.org/10.1016/j.cemconcomp.2012.05.007.

[48] S. Wan, X. Zhou, M. Zhou, Y. Han, Y. Chen, J. Geng, T. Wang, S. Xu, Z. Qiu, H. Hou, Hydration characteristics and modeling of ternary system of municipal solid wastes incineration fly ash-blast furnace slag-cement, Construct. Build. Mater. 180 (2018) 154–166, https://doi.org/10.1016/j.conbuildmat.2018.05.277.

[49] R.F. Feldman, G.G. Carette, V.M. Malhotra, Studies on mechanics of development of physical and mechanical properties of high-volume fly ash-cement pastes, Cement Concr. Compos. 12 (1990) 245–251, https://doi.org/10.1016/0958-9465(90)90003-G.

[50] M.K. Ardoğa, S.T. Erdoğan, M. Tokyay, Effect of particle size on early heat evolution of interground natural pozzolan blended cements, Construct. Build. Mater. 206 (2019) 210–218, https://doi.org/10.1016/j.conbuildmat.2019.02.055.

[51] C. Çetin, S.T. Erdoğan, M. Tokyay, Effect of particle size and slag content on the early hydration of interground blended cements, Cement Concr. Compos. 67 (2016) 39–49, https://doi.org/10.1016/j.cemconcomp.2015.12.001.

[52] S.E. Chidiac, D.K. Panesar, Evolution of mechanical properties of concrete containing ground granulated blast furnace slag and effects on the scaling resistance test at 28 days, Cement Concr. Compos. 30 (2008) 63–71, https://doi.org/10.1016/j.cemconcomp.2007.09.003.

[53] N. De Belie, J. Kratky, S. Van Vlierberghe, Influence of pozzolans and slag on the microstructure of partially carbonated cement paste by means of water vapour and nitrogen sorption experiments and BET calculations, Cement Concr. Res. 40 (2010) 1723–1733, https://doi.org/10.1016/j.cemconres.2010.08.014.

[54] J. Duchesne, M.A. Bérubé, The effectiveness of supplementary cementing materials in suppressing expansion due to ASR: another look at the reaction mechanisms part 1: concrete expansion and portlandite depletion, Cement Concr. Res. 24 (1994) 73–82, https://doi.org/10.1016/0008-8846(94)90084-1.

[55] S.M.R.A. Esfahani, S.A. Zareei, M. Madhkhan, F. Ameri, J. Rashidiani, R.A. Taheri, Mechanical and gamma-ray shielding properties and environmental benefits of concrete incorporating GGBFS and copper slag, J. Build. Eng. 33 (2021), 101615, https://doi.org/10.1016/j.jobe.2020.101615.

[56] T. Saeki, P.J.M. Monteiro, A model to predict the amount of calcium hydroxide in concrete containing mineral admixtures, Cement Concr. Res. 35 (2005) 1914–1921, https://doi.org/10.1016/j.cemconres.2004.11.018.

[57] C.B. Cheah, K.Y. Chung, M. Ramli, G.K. Lim, The engineering properties and microstructure development of cement mortar containing high volume of inter-grinded GGBS and PFA cured at ambient temperature, Construct. Build. Mater. 122 (2016) 683–693, https://doi.org/10.1016/j.conbuildmat.2016.06.105.
[58] P. Longuet, L. Burglen, A. Zelwer, The liquid phase of hydrated cement, Rev Matér Constr Trav Publics. 676 (1973) 35–41.
[59] B. Ersoy, S. Dikmen, T. Uygunoğlu, M. İçduygu, T. Kavas, A. Olgun, Effect of mixing water types on the time-dependent zeta potential of Portland cement paste, Sci. Eng. Compos. Mater. 20 (2013), https://doi.org/10.1515/secm-2012-0099.
[60] P. Hewlett, M. Liska, Lea's Chemistry of Cement and Concrete, Butterworth-Heinemann, 2019.
[61] V. Vishwakarma, D. Ramachandran, Green Concrete mix using solid waste and nanoparticles as alternatives – a review, Construct. Build. Mater. 162 (2018) 96–103, https://doi.org/10.1016/j.conbuildmat.2017.11.174.
[62] S. Tavasoli, M. Nili, B. Serpoush, Effect of GGBS on the frost resistance of self-consolidating concrete, Construct. Build. Mater. 165 (2018) 717–722, https://doi.org/10.1016/j.conbuildmat.2018.01.027.
[63] Finnish Meteorological Institute, n.d, https://en.ilmatieteenlaitos.fi/. (Accessed 12 May 2021).